Legionella pneumophila inhibits type I interferon signaling to avoid cell-intrinsic host cell defense.

C.N.S. Allen[1], D. A. Banks[1], M. Shuster[1], S. N. Vogel[2], T.J. O'Connor[3] and V. Briken[1]

[1] University of Maryland, Department of Cell Biology and Molecular Genetics

[2]Department of Microbiology and Immunology, University of Maryland School of Medicine, Baltimore, Maryland, USA

[3] Johns Hopkins University School of Medicine, Department of Biological Chemistry

Corresponding author: vbriken@umd.edu

Abstract:

The host type I interferon (IFN) response protects against *Legionella pneumophila* infections. Other bacterial pathogens inhibit type I IFN-mediated cell signaling; however, the interaction between this signaling pathway and *L. pneumophila* has not been well described. Here, we demonstrate that *L. pneumophila* inhibits the IFN-β signaling pathway but does not inhibit IFN-γ-mediated cell signaling. The addition of IFN-β to *L. pneumophila*-infected macrophages limited bacterial growth independently of NOS2 and reactive nitrogen species. The type IV secretion system of *L. pneumophila* is required to inhibit IFN-β-mediated cell signaling. Finally, we show that the inhibition of the IFN-β signaling pathway occurs downstream of STAT1 and STAT2 phosphorylation. In conclusion, our findings describe a novel host cell signaling pathway inhibited by *L. pneumophila* via its type IV secretion system.

28 **Introduction:**

29 *Legionella* species are ubiquitous in the environment and have adapted to survive within
30 freshwater amoebas (Rowbotham, 1980; Boamah et al., 2017). The bacteria rely on a type IV
31 secretion system (T4SS) named defective in organelle trafficking and intracellular multiplication
32 (Dot/Icm) to inject proteins into the host cell to manipulate host response pathways and increase
33 their chances of survival (Berger and Isberg, 1993; Brand et al., 1994; Segal and Shuman,
34 1998; Vogel et al., 1998). *Legionella* can infect a wide variety of amoeba species and, therefore
35 express multiple homologs of bacterial effectors to successfully modify the same host cell target
36 in various hosts (Park et al., 2020). Humans are accidental hosts that can be exposed to
37 *Legionella* via the aerosolization of contaminated water supplies, which may result in respiratory
38 infections (McDade et al., 1977).

39 Type I interferons (IFNs), such as IFN-β, bind to the heterodimeric interferon-α/β
40 receptor (IFNAR) and induce cell signaling, leading to the upregulation of hundreds of IFN-
41 stimulated genes (ISGs) (Stetson and Medzhitov, 2006; Lazear et al., 2019). Type I IFNs are
42 critical for host defense against viral pathogens (Stetson and Medzhitov, 2006; Lazear et al.,
43 2019). However, during bacterial infections the activity of type I IFNs is more complex, in some
44 cases mediating host resistance but in other cases increasing host susceptibility (Boxx and
45 Cheng, 2016; Peignier and Parker, 2021). *Legionella pneumophila* induces IFN-β production by
46 host cells via various cytosolic surveillance pathways, including the nucleic acid surveillance
47 pathway (Liu and Shin, 2019). Type I IFNs then signal through IFNARs expressed on the cell
48 surface of infected and bystander cells, contributing to *L. pneumophila* resistance, which has
49 been observed in mice (Lippmann et al., 2011). Multiple studies have demonstrated that cell-
50 intrinsic host defense mechanisms, including the production of nitric oxide (NO) (Plumlee et al.,
51 2009) and itaconic acid (Naujoks et al., 2016), are triggered by exogenous IFN-β and
52 subsequent IFNAR signaling during *ex vivo L. pneumophila* infections (Schiavoni et al., 2004;

53 Opitz et al., 2006; Plumlee et al., 2009; Majoros et al., 2016). Thus, the IFN-β response plays a
54 role in determining the outcome of *L. pneumophila* infections.
55 Here, we demonstrate that *L. pneumophila* can inhibit IFN-β-mediated cell signaling, and
56 this inhibition occurs downstream of the phosphorylation of STAT1 and STAT2. Additionally, we
57 show that the ability to reduce IFN-β signaling depends on the T4SS of *L. pneumophila* and is
58 thus likely mediated by a secreted effector(s).
59

60 **Materials and Methods:**

61 **Cell culture and Mice**

62 RAW 264.7 and RAW-Lucia ISG-KO-IRF3 cells (InvivoGen, rawl-koirf3) were grown in
63 DMEM supplemented with 10% heat-inactivated fetal bovine serum (FBS). RAW-Lucia ISG-KO-
64 IRF3 cells were plated in FBS-free DMEM 16 hours before the infection since the absence of
65 FBS reduces the background activation of the integrated ISRE-Luciferase gene cassette.

66 THP-1 cells were purchased from ATCC and were maintained at 37°C and 5% CO_2 in
67 RPMI (ATCC) supplemented with 10% heat-inactivated FBS. For differentiation, THP-1 cells
68 were treated with 50 ng/ml of phorbol 12-myristate 13-acetate (PMA) for two days. The media
69 was then replaced and cells were cultured for two more days before infections.

70 Bone marrow-derived macrophages (BMDMs) were prepared from bone marrow cells
71 flushed from the tibias and femurs of wild-type, *Ifnb*$^{-/-}$, and *Nos2*$^{-/-}$ mice. The BMDMs were
72 cultured in Gibco Dulbecco's Modified Eagle Medium (DMEM) supplemented with 10% heat-
73 inactivated FBS, 1% penicillin/streptomycin, and 20% L929 conditioned medium for six days
74 prior to infection. L929 conditioned medium was used for all the BMDM infection experiments.
75 *Ifnb*$^{-/-}$ mice were originally obtained from Dr. E. Fish (University of Toronto) and have been
76 previously described (Deonarain et al., 2000). 57BL/6J (JAX SO: 5530121) and *Nos2*$^{-/-}$ (JAX
77 SO: 5530126) mice were obtained from the Jackson Laboratory. All mice used for BMDMs were
78 female.

79

80 **Ethics statement**

81 All animals were handled in accordance with the NIH guidelines for the housing and care
82 of laboratory animals. Studies were approved by the Institutional Animal Care and Use
83 Committee at the University of Maryland.

84

85 **Bacteria**

86 *L. pneumophila* Philadelphia-1 strain Lp02 was cultured at 37°C in liquid N-(2-
87 87Acetamido)-2-aminoethanesulfonic acid (ACES)-buffered yeast extract (AYE) medium or on
88 solid charcoal ACES-buffered yeast extract (CYET) containing 0.135 mg/ml L-cysteine (Sigma),
89 0.4 mg/ml iron(III) nitrate (Sigma), and 0.1 mg/ml thymidine (Sigma). The *L. pneumophila* Lp02
90 *dotA deficient* mutant (Δ*dotA)* was previously described (Berger and Isberg, 1993).
91 Heat inactivation of *L. pneumophila and* Δ*dotA L. pneumophila* was achieved based on
92 a previous protocol (Allegra et al., 2011). Briefly, the bacteria were incubated in a water bath at
93 70°C for 30 minutes prior to the infections.
94 **Cellular infections**
95 *L. pneumophila* were grown in AYE medium to the post-exponential phase (OD_{600} = 3.7–
96 4.1). RAW-Lucia ISG-KO-IRF3 cells, differentiated THP-1 cells, and BMDMs were infected with
97 *L. pneumophila* for one hour at the indicated multiplicity of infections (MOI). The cells were
98 washed three times with phosphate-buffered saline (PBS) and incubated in DMEM media
99 supplemented with or without IFN-β for the given time.
100
101 **IFN-β enzyme-linked immunosorbent assay (ELISA)**
102 The levels of secreted IFN-β were measured by an IFN-β enzyme-linked immunosorbent
103 assay (ELISA) (R&D Systems) following the manufacturer's protocol. RAW 264.7 cells were
104 infected with *L. pneumophila* at an MOI of 0.05 for one hour. After one hour, the media was
105 removed, the cells were rinsed three times with growth media, and fresh growth media was
106 added. The supernatants of the infected and uninfected cells were collected at 24-, 48-, 72-, and
107 96-hours post-infection (h.p.i). IFN-β levels were measured by a plate reader (BioTek ELx800).
108
109 **Luciferase Reporter Assay**
110 RAW-Lucia ISG-KO-IRF3 cells were infected with *L. pneumophila* at an MOI of 10 for
111 one hour. After one hour, the cells were rinsed three times with media and then incubated in

112 fresh growth media. At the indicated concentrations, IFN-β (R&D Systems) or IFN-γ (R&D
113 Systems) was added to the post-infection media at 0 h.p.i. The supernatant from the infected
114 and uninfected cells was collected, and the amount of type I IFN signaling was indirectly
115 measured using QUANTI-Luc Gold, following the manufacturer's protocol.
116
117 **qRT-PCR Assay**
118 Total RNA was extracted using a GeneJet RNA Purification Kit (Thermo Scientific). A
119 NanoDrop 8000 spectrophotometer (Thermo Scientific) was used to determine the purity and
120 concentration of the RNA. cDNA was synthesized from collected RNA using SuperScript IV
121 VILO cDNA Master Mix with ezDNase (Invitrogen). The following primers were used: BST2
122 (tetherin): (F) 5′-caaactcctgcaacctgaccgt -3′; (R) 5′-ctcctggttcagcttcgtgact-3′ and beta actin: (F)
123 5′-cattgctgacaggatgcagaagg-3′; (R) 5′-tgctggaaggtggacagtgagg-3′. All analyses were performed
124 using FastStart Universal SYBR Green (Roche) according to the manufacturer's instructions.
125 The relative mRNA quantitation was done using the comparative ΔΔCt method, and all results
126 are compared to the control group and loading control beta actin.
127
128 **Cell Death AK Release Assay**
129 A ToxiLight BioAssay Kit (Lonza) was used to determine cell death. This assay
130 measures the amount of adenylate kinase (AK) in the cellular supernatant released upon cell
131 membrane damage. The assay was performed following the manufacturer's protocol. Briefly, 20
132 µl of cellular supernatants from the infected and uninfected cell cultures were added to a 96-well
133 plate. Then, 100 µl of the AKDR solution from the kit was added to each well and incubated for
134 five minutes. The plate was then read using a microplate reader (BioTek).
135 **Bacterial Survival**
136 For bacterial survival assays, *L. pneumophila* used for infections was grown to the post-
137 exponential phase (OD_{600} = 3.8–4.0). Wild-type, *Nos2*$^{-/-}$, and *Ifna*$^{-/-}$ BMDMs were infected with *L.*

138 *pneumophila* at an MOI of 1 for one hour. After one hour, the cells were rinsed three times, and
139 the media was replaced with BMDM growth media. At the provided time points, saponin was
140 added to the cells to achieve a final concentration of 0.02% (w/v), and the cells were incubated
141 for ten minutes at 37°C. The medium was then harvested, and 100 µL of sterile water was
142 added to the wells. The water was then harvested and mixed with the original harvested media.
143 The bacteria were counted based on colony-forming units (CFUs) from plating diluted cellular
144 lysates on CYE medium agar plates.
145
146 **Antibody neutralization**
147 Antibody neutralization studies were performed using *InVivo*Plus anti-mouse IFNAR1
148 and *InVivo*MAB mouse IgG1 isotype control antibodies (Bio X Cell). Antibodies were added to
149 the infected cells at 0 h.p.i. at a final concentration of 20 µg/ml. The bacterial survival study was
150 performed using wild-type 57BL/6J BMDMs. Briefly, BMDMs were infected with *L. pneumophila*
151 at an MOI of 1 for one hour, then the cells were rinsed three times, and the media was replaced.
152 At the provided time points, saponin was added to the cells to achieve a final concentration of
153 0.02% (w/v), and the cells were incubated for ten minutes at 37°C. The medium was then
154 harvested, and 100 µL of sterile water was added, harvested, and mixed with the original
155 harvested media. The bacteria were counted based on colony-forming units (CFUs) from plating
156 diluted cellular lysates on CYE medium agar plates.
157
158 **NO assay**
159 The production of NO in response to IFN-β was quantified using a Griess assay kit
160 (Promega) following the manufacturer's protocol. Briefly, 50 µL of supernatant from the infected
161 cells with or without IFN-β at the indicated time points was added to wells in triplicate, mixed
162 with 50 µL of the Sulfanilamide solution, and incubated at room temperature for ten minutes.
163 Then, 50 µL of the NED solution was added and incubated at room temperature for ten minutes.

164 The production of nitrite, a derivative of NO, was measured at 548 nm using a microplate reader
165 (BioTek). The nitrite concentration was determined using a sodium nitrite standard curve.
166
167 **Flow Cytometry**
168 Differentiated THP-1 cells were infected with GFP-positive *L. pneumophila or L.*
169 *pneumophila* Δ*dotA* at an MOI of 10 for one hour. After infection, the media was removed, cells
170 were rinsed three times with fresh media, and fresh growth media was added and incubated for
171 30 minutes (STAT1 and STAT2) or 20 hours (tetherin). At collection, the medium was removed,
172 and Cellstripper (Corning) was added to detach the cells from the plate surface. The cells were
173 centrifuged at 425 x g for three minutes at 4°C. The supernatant was removed, and the cell
174 pellet was rinsed twice with 1 ml of PBS.
175 For live/dead staining, a LIVE/DEAD Yellow Fixable Dead Stain kit (Thermo Fisher
176 Scientific) was used for the anti-tetherin flow cytometry, and a LIVE/DEAD Near-IR Fixable
177 Dead Stain kit (Thermo Fisher Scientific) was used for the STAT1 and STAT2 flow cytometry
178 following the manufacturer's protocol. Briefly, the collected and rinsed cell pellets were
179 resuspended in 1 ml of PBS, and 1 µL of the fluorescent reactive dye from the kit was added to
180 each sample. The cells were then incubated in the dark for 30 minutes. The cells were then
181 centrifuged at 425 x g for three minutes at 4°C, rinsed with 1 ml of PBS, and centrifuged two
182 additional times. After the last centrifugation, the cell pellets were resuspended in the flow buffer
183 (PBS with 0.5 % BSA).
184 For the cell surface staining for the tetherin flow cytometry, the cell pellets were
185 resuspended in 50 µL of flow buffer. Human TruStain FcX (BioLegend) was added at a 1:10
186 dilution, and the cells were briefly vortexed. The cells were incubated for ten minutes. Next, 50
187 µL of the stain cocktail (1x Brillant Stain Buffer [BD Bioscience] and 5 µL per sample of APC
188 anti-human CD317 (BST2, Tetherin) antibody [BioLegend]) was added to each sample. The
189 samples were then incubated for one hour on ice in the dark. After the incubation, 1 ml of flow

190 buffer was added to the samples, centrifuged at 425 x g for three minutes at 4°C, rinsed with 1
191 ml of flow buffer, and centrifuged two more times. The cells were resuspended in 4% PFA
192 before running the samples.

193 For the intercellular staining for STAT1 and STAT2, the cell pellets were resuspended in
194 100 µL of 4% PFA for 15 minutes on ice. The cells were centrifuged at 425 x g for three minutes
195 at 4°C and rinsed with ice-cold PBS. For permeabilization, 1 ml of ice-cold 100% methanol was
196 added to the cells on ice. The cells were incubated for ten minutes on ice. The cells were then
197 centrifuged at 425 x g for three minutes at 4°C and rinsed with ice-cold PBS. The cell pellets
198 were resuspended in 50 µL of flow buffer. Human TruStain FcX (BioLegend) was added at a
199 1:10 dilution, and the cells were briefly vortexed. The cells were incubated for ten minutes. Next,
200 50 µL of the stain cocktail (1x Brillant Stain Buffer [BD Bioscience] and either 5 µL per sample of
201 Alexa Flour 647 Anti-Total Stat1 [N-Terminus] [BD Biosciences] and 5 µL per sample of PE anti-
202 STAT1 Phospho [Tyr701] [BioLegend]; or 2 µL per sample of Stat2 [D9J7L] Rabbit mAb [PE]
203 [Cell Signaling Technology] and 2 µL per sample of P-Stat2 [P-690] Rabbit mAb [Alexa 647]
204 [Cell Signaling Technology]) was added to each sample. The samples were then incubated for
205 one hour on ice in the dark. After the incubation, 1 ml of flow buffer was added to the samples,
206 centrifuged at 425 x g for three minutes at 4°C, rinsed with 1 ml of flow buffer, and centrifuged
207 two more times. The cells were then resuspended in 4% PFA prior to running the samples.

208 **Statistical Analysis**

209 All statistical analyses were performed using GraphPad 9.0. For all the experiments, the
210 data are shown as the mean ± standard deviation (*SD*) of three biological replicates unless
211 otherwise noted. Significance is indicated by a *p*-value less than or equal to 0.05.

212 **Results:**

213 To test how much IFN-β is produced during *L. pneumophila* infections, RAW 264.7 cells
214 were infected with *L. pneumophila* at an MOI of 0.05 for one hour. After one hour of infection,
215 the cells were rinsed, and fresh media was added. The amount of secreted IFN-β was
216 measured at 24-hour intervals via ELISA. Each data point is obtained from the average of three
217 technical replicates and represents an independent experiment. After 24 hours, 163.5 ± 55.2
218 pg/ml of IFN-β was detected, a ten-fold increase compared with the uninfected cells, and the
219 IFN-β production stayed constant until 48 h.p.i. At 72 h.p.i., the level of IFN-β increased to 342.4
220 ± 103.9 pg/ml and continued to rise to 460.9 ± 109.5 pg/ml by 96 h.p.i. (Figure 1A). These
221 results indicate that *L. pneumophila* induces IFN-β production in RAW 264.7 macrophages and
222 that IFN-β accumulates over time after the infection.

223 Since it has been previously reported that *Mycobacterium tuberculosis* and *Shigella*
224 *sonnei* inhibit IFNAR signaling in infected cells (Banks et al., 2019a; Alphonse et al., 2022), we
225 wanted to determine if *L. pneumophila* also inhibits type I interferon signaling. RAW-Lucia ISG-
226 KO-IRF3 cells were used for these studies since they are deficient in *Irf3* and consequently
227 infections with *L. pneumophilia* will not induce the production of endogenous IFN-β. Hence, the
228 only IFN-β-mediated cell signaling detected by the IFN-β-inducible reporter gene is that of the
229 IFN-β added exogenously to the cells. Cells infected or not with *L. pneumophila* at an MOI of 10
230 were cultured with increasing amounts of IFN-β (200–2000 pg/ml) for 20 hours to measure the
231 effect *L. pneumophila* has on IFN-β-mediated cell signaling. The secretion of luciferase into the
232 supernatant correlates with the activity of the IFN-β responsive promotor. The secreted
233 luciferase was measured via a chemiluminescence assay and results are expressed in relative
234 light units (RLU). Cells infected with *L. pneumophila* had lower levels of IFN-β-associated gene
235 expression at all the doses of IFN-β tested when compared to the uninfected, untreated cells
236 (Figure 1B). At the lower doses of IFN-β (200 and 400 pg/ml) a fold change of 0.25 relative to
237 the uninfected cells was measured which changed to 0.8 at the highest IFN-β dose of 2000

238 pg/ml (Figure 1C). The IFN-β signaling pathway inhibition was reduced in a dose-dependent
239 manner, suggesting that as the IFN-β concentration increases, the ability of *L. pneumophila* to
240 impede the signaling pathway is overwhelmed.

241 The IFN-β and IFN-γ signal transduction pathways share some of their intracellular
242 signaling components, and thus, we asked if *L. pneumophila* can also inhibit IFN-γ signaling.
243 The RAW-Lucia ISG-KO-IRF3 reporter construct is also induced by IFN-γ signaling and could
244 thus serve as a model to study the potential of *L. pneumophila* to inhibit IFN-γ signaling.
245 Increasing amounts of IFN-γ (200–2000 pg/ml) were added to *L. pneumophila*-infected or
246 uninfected cells (MOI of 10), and the luciferase production was analyzed (Figures 1D and E).
247 Overall, there was no reduction in the IFN-γ response in the infected cells; however, at IFN-γ
248 doses of 1000 and 2000 pg/ml, there was a significant increase in transcription response in the
249 *L. pneumophila*-infected cells compared with the uninfected cells (Figures 1D and E). These
250 results indicate that *L. pneumophila* partially inhibits IFN-β signaling while not affecting IFN-γ
251 signaling.

252 *L. pneumophilia* can reduce host protein synthesis via the secretion of multiple effectors
253 (Belyi et al., 2006; Shen et al., 2009; Fontana et al., 2011; Moss et al., 2019). To determine if
254 the decrease in the IFN-β signaling in *L. pneumophila*-infected RAW-Lucia ISG-KO-IRF3 cells
255 was due to decreased global protein production, a q-RT-PCR for the mRNA of the IFN-β-
256 inducible gene tetherin (BST-2) was performed. In RAW-Lucia ISG-KO-IRF3 cells infected or
257 not with *L. pneumophila* at an MOI of 10, treated or not with IFN-β and cells were harvested for
258 mRNA extraction at 4 hours post infection. The level of tetherin mRNA in the infected cells, not
259 treated with IFN-β was three-fold higher than in the uninfected RAW-Lucia ISG-KO-IRF3 not
260 treated with IFN-β. The induction of tetherin mRNA in the infected RAW-Lucia ISG-KO-IRF3
261 cells treated with IFN-β (1000 pg/ml) was significantly less than the induction of tetherin mRNA
262 in the uninfected RAW-Lucia ISG-KO-IRF3 treated with IFN-β (Figure 2A). This result suggests

263 that the decrease in IFN-β signaling pathway is due to an inhibition of an event upstream of
264 transcription initiation. It also shows that the observed inhibition in the generation of luciferase in
265 the reporter cells is not due to an inhibition of overall protein synthesis due to *L. pneumophila*
266 infections.

267 An AK release assay was performed to test if the decrease in the IFN-β-mediated
268 luciferase production was due to a decrease in the total number of reporter cells due to
269 increased cell death. After 20 h.p.i, compared with the uninfected, non-IFN-β treated RAW-Lucia
270 ISG-KO-IRF3 cells, there was no significant increase in cell death in the *L. pneumophila*-
271 infected (MOI of 10) IFN-β treated cells (Figure 2B). This result suggests that the decrease in
272 luciferase in the *L. pneumophila*-infected RAW-Lucia ISG-KO-IRF3 cells was not from
273 decreased cell counts via increased cell death.

274 IFN-β has been shown to contribute to the clearance of *L. pneumophila* in mice
275 (Lippmann et al., 2011) and in *ex vivo* infected BMDMs (Schiavoni et al., 2004; Plumlee et al.,
276 2009; Lippmann et al., 2011). *Ifnb*$^{-/-}$-derived BMDMs were infected with *L. pneumophila* and
277 treated with IFN-β to determine the effects of IFN-β on bacterial survival within macrophages.
278 We used *Ifnb*$^{-/-}$-derived BMDMs to observe the effects of exogenous IFN-β without the
279 production of endogenous IFN-β in response to the *L. pneumophila* infection (Plumlee et al.,
280 2009; Lippmann et al., 2011). Infected cells were treated with or without an IFNAR1-neutralizing
281 antibody or an isotype antibody to demonstrate the specificity of the IFN-β treatment due to
282 IFNAR signaling. The *Ifnb*$^{-/-}$-derived BMDMs were infected with *L. pneumophila* at an MOI of 1,
283 and then 20 μg/ml of the IFNAR1-neutralizing or isotype control antibodies were added. The
284 IFN-β treated groups were then treated with 1000 pg/ml IFN-β. The addition of IFN-β to the *Ifnb*$^{-}$
285 $^{/-}$-derived BMDMs did not affect the growth of the bacteria for the first two time points (24 and 48
286 h.p.i.) but at 72 and 96 h.p.i. there was a significant reduction in the CFUs in the isotype IFN-β-
287 treated cells compared with the untreated isotype cells (Figure 3A). However, blocking the
288 IFNAR receptor by the IFNAR1-neutralizing antibodies inhibited the IFN-β-mediated reduction in

289 the CFUs (Figure 3A). These results indicate that IFN-β plays a role in the growth inhibition of *L.*
290 *pneumophila* in macrophages and that this inhibition is dependent on signaling through the
291 IFNAR1 receptor.

292 Next, we investigated the role of NO production on host protection during IFN-β
293 treatment. The NO production was analyzed using a Griess assay, which detects nitrite as a
294 proxy for the induced production of NO. *L. pneumophila*-infected (MOI of 10) RAW-Lucia ISG-
295 KO-IRF3 cells had a slight increase in nitrite levels in the IFN-β-treated cells (1000 pg/ml)
296 compared with untreated cells at 24 h.p.i. (Figure 3B). After 48 hours, the IFN-β treatment
297 increased the nitrite level to about 18 μM; however, the nitrite level in the untreated cells was
298 about 5 μM. The IFN-β treatment led to nitrite production of about 25 μM at 96 hours, whereas
299 the level in the untreated cells remained low and was around 8 μM (Figure 3B). These results
300 show that IFN-β signaling induced NO production in the RAW-Lucia ISG-KO-IRF3 cells and that
301 the production of NO is reduced in cells infected with *L. pneumophila*.

302 To determine if the reduced NO production influenced the clearance of *L. pneumophila,*
303 wild-type and *Nos2*$^{-/-}$ BMDMs were infected with *L. pneumophila* at an MOI of 1 and treated with
304 or without IFN-β (1000 pg/ml). The *Nos2*$^{-/-}$ BMDMs not treated with IFN-β had the greatest
305 amount of bacterial growth. The wild-type IFN-β untreated BMDMs had significantly reduced
306 bacterial growth over all the measured time points compared with the *Nos2*$^{-/-}$ untreated BMDMs
307 (Figure 3C). This result suggests that Nos2 provides some protection against *L. pneumophila* in
308 an IFN-β independent pathway. The *Nos2*$^{-/-}$ and wild-type BMDMs treated with IFN-β had
309 significantly decreased bacterial survival compared with the BMDMs not treated with IFN-β;
310 however, there was no significant difference between the *Nos2*$^{-/-}$ BMDMs and the wild-type
311 BMDMs treated with IFN-β (Figure 3C). This lack of significance in bacterial survival between
312 the *Nos2*$^{-/-}$ BMDMs and the wild-type BMDMs treated with IFN-β suggests that the growth
313 inhibition of *L. pneumophila* observed with IFN-β is Nos2 independent.

314 To further test the role of reactive nitrogen species (RNS) in the clearance of *L.*
315 *pneumophila* in response to IFN-β, the iNOS inhibitor L-NMMA was used. First, it was
316 determined that L-NMMA had a dose-dependent effect on the nitrite production of wild-type
317 BMDMs treated with IFN-β (1000 pg/ml) after 20 hours. At the highest dose of L-NMMA (12
318 μM), the nitrite production was approximately 15% of the nitrite produced by the untreated cells
319 (Supplementary Figure 1A). L-NMMA (12 μM) was also determined to have no effect on *L.*
320 *pneumophila* cell growth rate (Supplementary Figure 1B). Wild-type BMDMs were infected with
321 *L. pneumophila* at an MOI of 1 and treated with or without IFN-β (1000 pg/ml) and with a solvent
322 control (DMSO) or 12 μM of L-NMMA to observe the effect that NO production has on the
323 survival of *L. pneumophila* (Figure 3D). The L-NMMA treated and IFN-β untreated BMDMs and
324 the untreated BMDMS had similar bacterial growth at all the tested time points. However, the L-
325 NMMA and IFN-β treated, and the only IFN-β treated BMDMs, had significantly decreased
326 bacterial survival compared with the BMDMs not treated with IFN-β (Figure 3D). This decreased
327 bacterial survival was similar for the L-NMMA and IFN-β treated and the only IFN-β treated
328 BMDMs. This result further suggests that the clearance of *L. pneumophila* observed with IFN-β
329 is independent of RNS.
330
331 *L. pneumophila* T4SS Dot/Icm is a critical virulence factor that deploys effector proteins
332 to the host cell to manipulate host cellular processes (Berger and Isberg, 1993; Brand et al.,
333 1994; Segal and Shuman, 1998; Vogel et al., 1998). One mechanism by which *L. pneumophila*
334 might inhibit IFN-β signaling is through the activity of a secreted effector. To test this, an *L.*
335 *pneumophila dotA* deficient mutant (Δ*dotA*) was used to explore the importance of the Dot/Icm
336 system and, thus, the possibility that an effector is involved in inhibiting the IFN-β signaling
337 pathway. RAW-Lucia ISG-KO-IRF3 cells were infected with wild-type *L. pneumophila* or the
338 Δ*dotA* mutant *L. pneumophila* at an MOI of 10 and were treated with 0, 600, 1000, or 2000

339 pg/ml of IFN-β for 20 hours (Figure 4A). The IFN-β-mediated signaling was reduced in the cells
340 infected with the wild-type bacteria to approximately 60% of uninfected, IFN-β-treated cells, for
341 all the tested IFN-β concentrations (Figure 4A). In contrast, the Δ*dotA* mutant did not reduce the
342 IFN-β-mediated signaling as much as the wild-type *L. pneumophila* (Figure 4A). In addition to
343 the wild-type and Δ*dotA* mutant, RAW-Lucia ISG-KO-IRF3 cells were infected with heat-
344 inactivated wild-type or Δ*dotA* mutant bacteria at an MOI of 10 to explore if the inhibition of the
345 IFN-β signaling pathway requires live bacteria or if the inhibition is a result of pre-existing heat
346 resistant bacterial lipids. The two heat-inactivated bacterial strains did not inhibit IFN-β signaling
347 compared with the uninfected Raw-Lucia ISG-KO-IRF3 cells (Figure 4A). Overall, these results
348 suggest that the inhibition of the IFN-β pathway results from the activity of an effector secreted
349 through the Dot/Icm T4SS.

350 Next, the role of the T4SS on the capacity of infected cells to produce NO upon IFN-β
351 stimulation was analyzed. Uninfected RAW-Lucia ISG-KO-IRF3 cells treated with 100 ng/ml
352 LPS and 1000 pg/ml IFN-β were used as a positive control. RAW-Lucia ISG-KO-IRF3 cells were
353 infected with either wild-type *L. pneumophila* or Δdot*A* mutant *L. pneumophila* at an MOI of 10
354 and treated with IFN-β (1000 pg/ml). The wild-type *L. pneumophila*-infected cells had
355 significantly less NO production than the Δdot*A* mutant-infected cells or the positive control cells
356 (Figure 4B). The level of NO produced was not significantly different between the Δ*dotA* mutant
357 *L. pneumophila*-infected cells and the positive control. Overall, these results demonstrate that
358 the Dot/Icm T4SS is necessary for the bacteria to inhibit IFN-β-mediated cell signaling and
359 suggest that one or more *L. pneumophila* effectors secreted into the host cell are responsible for
360 inhibiting the IFN-β signaling pathway in murine cells.

361 To explore if the IFN-β signaling inhibition caused by *L. pneumophila* seen in the murine
362 cells also occurs in human cells, the human monocyte cell line THP-1 was used. THP-1 cells
363 were differentiated into macrophages using PMA for 48 hours and then cultured in media
364 without PMA for 48 hours, before infection with bacteria. The effects of *L. pneumophila* on the

365 IFN-β signaling pathway were observed by flow cytometry measuring the cell surface tetherin
366 levels. For these experiments, GFP wild-type and GFP Δ*dotA* mutant *L. pneumophila* were
367 used, which allowed us to specifically study *L. pneumophila*-infected THP-1 cells. The gating
368 strategy for the flow cytometry analysis was first to define the cell population (SSC/FSC), then
369 gate on single-cells, live cells, and finally the GFP-positive, infected cells (Supplementary Figure
370 2). The tetherin antibody showed an increase in mean fluorescence intensity (MFI) when
371 compared with the isotype control (Supplementary Figure 3A), and the GFP signal did not
372 influence the APC tetherin antibody signal (Supplementary Figure 3B). Differentiated THP-1
373 cells were infected with wild-type or Δ*dotA* mutant *L. pneumophila* at an MOI of 10. Then, the
374 infected and uninfected cells were left untreated or treated with IFN-β (10 ng/ml). After 20 hours,
375 the uninfected cells treated with IFN-β had roughly a three-fold increase in tetherin-staining MFI
376 compared with the uninfected, untreated cells (Figure 5A). The wild-type *L. pneumophila*-
377 infected, IFN-β treated cells had less of an induction of tetherin staining (1.5-fold over
378 uninfected, untreated) compared to the three-fold induction of the uninfected, IFN-β-treated
379 cells. However, the Δ*dotA* mutant *L. pneumophila*-infected, IFN-β treated cells had no significant
380 difference in the tetherin cell surface expression when compared with the uninfected, IFN-β-
381 treated cells (Figure 5A). These results show that *L. pneumophila* inhibits the IFN-β signaling
382 pathway in a T4SS-dependent manner in human macrophage-like cells.
383 The activation of STAT1 and STAT2 via phosphorylation after IFN-β binding to IFNAR1
384 is an important step in the IFNAR signaling pathway and is important for the suppression of *L.*
385 *pneumophila* growth (Abdul-Sater et al., 2015). In order to assess if *L. pneumophila* infections
386 inhibit STAT1 or STAT2 phosphorylation, the levels of phospho-STAT1 and phospho-STAT2 in
387 *L. pneumophila*-infected THP-1 cells treated with IFN-β were measured by flow cytometry. The
388 total STAT1, phospho-STAT1, total STAT2, and phospho-STAT2 specific antibodies showed
389 good increases in MFI when compared with the isotype controls (Supplementary Figure 4), and
390 for each of these antibody stainings, the GFP signal of the *L. pneumophila* bacteria did not

391 cross over (Supplementary Figure 4). Differentiated THP-1 cells were infected with wild-type or
392 Δ*dotA* mutant *L. pneumophila* at an MOI of 10. Next, the infected and uninfected cells were left
393 untreated or treated with IFN-β (10 ng/ml) for 30 minutes. The uninfected, IFN-β-treated cells
394 had about a nine-fold increase in phospho-STAT1 MFI and a six-fold increase in phospho-
395 STAT2 MFI when compared with the uninfected, untreated cells, indicating that IFN-β increased
396 the phosphorylation of these two proteins (Figures 5B and 5C). The wild-type *L. pneumophila*
397 and Δ*dotA* mutant *L. pneumophila* infected, untreated cells had increased phospho-STAT1 (Lp:
398 6-fold change, LpΔ: 3-fold change) and phospho-STAT2 (Lp: 2-fold change, LpΔ: 2-fold change)
399 levels compared with the uninfected, untreated cells, probably due to endogenous expression of
400 IFN-β after the infection (Figures 5B and 5C). Cells infected with wild-type *L. pneumophila* and
401 treated with IFN-β had a similar fold change increase in STAT1 phosphorylation compared to
402 uninfected, IFN-β-treated cells (about 9 to 10-fold for both). However, these cells showed a
403 significantly stronger increase (10-fold) in the level of phospho-STAT2 when compared with the
404 uninfected, IFN-β-treated cells (5-fold) (Figures 5B and 5C). Cells infected with the Δ*dotA*
405 mutant and treated with IFN-β had significantly increased phospho-STAT1 and phospho-STAT2
406 levels compared with the uninfected, IFN-β treated cells (Figures 5B and 5C). The levels of total
407 STAT1 and STAT2 were significantly changed in some conditions but overall, the magnitude of
408 these changes were minor (Supplementary Figure 5A and B). These results suggest that the
409 IFN-β signaling pathway inhibition caused by *L. pneumophila* is downstream of the
410 phosphorylation of STAT1 and STAT2.
411

412 **Discussion**

413 Type I IFNs have mainly been shown to play a protective role during viral infections
414 (Lazear et al., 2019); however, the role of type I IFNs is more complex in bacterial infections
415 since IFN-β has been shown to produce protective and detrimental effects depending on the
416 bacterial pathogen (Boxx and Cheng, 2016; Peignier and Parker, 2021). We demonstrate that

417 IFN-β plays a protective role against an *L. pneumophila* infection and contributes to the
418 clearance of *L. pneumophila* in BMDMs (Fig. 3). This observation aligns with previous studies,
419 which have shown that type I IFN protects against *L. pneumophila* infections in an IFN-γ-
420 independent way during *ex vivo* and *in vivo* infections (Schiavoni et al., 2004; Plumlee et al.,
421 2009; Lippmann et al., 2011; Abdul-Sater et al., 2015). NOS2/iNOS generates NO and
422 subsequently reactive nitrogen intermediates, which have cell-intrinsic, anti-bacterial activity
423 against the growth of many bacterial pathogens but seem to be mostly ineffective against *L.*
424 *pneumophila* (Gebran et al., 1994; Akamine et al., 2007; Plumlee et al., 2009; Naujoks et al.,
425 2016; Price et al., 2019), Accordingly, we did not observe any difference in bacterial growth
426 between the *Nos2*$^{-/-}$ BMDMs and the wild-type BMDMs treated with IFN-β. One possibility for
427 this lack of difference in bacterial survival could be redundancy in signaling pathways similar to
428 what has been shown for the protective activity of IFN-γ against *L. pneumophila,* where IRG1
429 and NOS2 compensate for the loss of one another (Price et al., 2019). The IFN-β/IRG-1
430 pathway mediates increased itaconic acid production, which targets *L. pneumophila*-containing
431 vacuoles and acts as a bactericide (Naujoks et al., 2016). Another possibility is that, unlike IFN-
432 γ, the anti-bacterial effect of IFN-β is RNS independent.
433 Previous studies have identified bacterial pathogens that inhibit IFN-β signaling. For
434 instance, *M. tuberculosis* inhibits IFN-β signaling by limiting the activation of IFNAR-associated
435 tyrosine kinase (Banks et al., 2019a). *S. sonnei* inhibits IFN signaling through the secreted
436 effector OspC, which binds to the host cell calmodulin, inhibiting calmodulin kinase II and
437 STAT1 phosphorylation (Alphonse et al., 2022). *L. pneumophila* inhibits host cell IFN-β
438 production via the T4SS-secreted effector Sdha (Monroe et al., 2009). However, we, to our best
439 knowledge, are the first to demonstrate that *L. pneumophila* employs mechanisms to inhibit IFN-
440 β signaling. Our results suggest that *L. pneumophila* secretes an effector(s) to inhibit the IFN-β
441 response since the T4SS-deficient mutant failed to inhibit IFN-β signaling (Figs. 4A, 5A).
442 Furthermore, *L. pneumophila* inhibits IFN-β signaling downstream of STAT1 and STAT2

443 phosphorylation since they are not downregulated upon *L. pneumophila* infection (Figs. 5B, 5C),
444 which is different from *M. tuberculosis*- and *S. sonnei*-mediated inhibition (Banks et al., 2019b;
445 Alphonse et al., 2022).

446 Humans are an accidental host for *L. pneumophila,* and so *L. pneumophila* has primarily
447 adapted to survive in amoebas and not in human macrophages. Amoebas do not have an
448 equivalent receptor to IFNAR or any class of receptors associated with tyrosine kinases
449 (Goldberg et al., 2006). The evolutionary advantage for *L. pneumophila* to inhibit IFNAR-
450 signaling when amoebas lack equivalent receptors is thus unclear. However, amoebas, such as
451 *Dictyostelium sp.* and *Acanthamoeba sp.,* express a homolog to mammalian STAT proteins
452 (Kawata et al., 1997; Kicinska et al., 2014). In particular, the amoebal STAT protein is closely
453 related to the human and mouse STAT2 protein (Kicinska et al., 2014), which is the STAT
454 isoform involved in type I but not type II IFN signaling (Villarino et al., 2020). This could
455 potentially explain why *L. pneumophila* can inhibit type I but not type II IFN signaling.

456 SH2 domains are the primary protein domain responsible for binding tyrosine-
457 phosphorylated targets involved in tyrosine kinase signaling cascades, such as the STAT1 and
458 STAT2 cascade (Schlessinger and Lemmon, 2003). Interestingly, *L. pneumophila* encodes for
459 84 proteins that contain an SH2 domain, and these SH2 domains, while lacking pocket
460 specificity, bind mammalian phosphorylated tyrosines with strong affinities (Kaneko et al., 2018).
461 Consequently, *L. pneumophila* could have evolved mechanisms to suppress amoebal STAT-
462 mediated transcriptional regulation, allowing for the growth of *L. pneumophila* in amoebas, and
463 serendipitously, this mechanism also inhibits mammalian STAT2-mediated transcriptional
464 regulation. Due to the homology of mammalian STAT2 with the amoeba STAT and the SH2
465 domains found in *L. pneumophila* proteins (Kicinska et al., 2014), we hypothesize that IFNAR
466 signaling could be inhibited at the STAT2 level after the phosphorylation of STAT2 via
467 interactions with an SH2 domain found in an *L. pneumophila* protein. This could potentially block
468 the association of STAT2 with STAT1 and IRF9, which is required to form the active ISGF3

complex. However, further studies are needed to test this hypothesis and identify the putative *L. pneumophila*-secreted effector responsible for the inhibition of IFN-β signaling.

Acknowledgements

C.N.S.A., D.A.B., M.S. and V.B. were supported by grants R21AI142396 and R21 AI151973. S.A.V. by grant R01 AI123371. M.S. was supported by “The Stefanie & Richard Vogel Graduate Student Award” and T32 AI089621.

Fig. 1

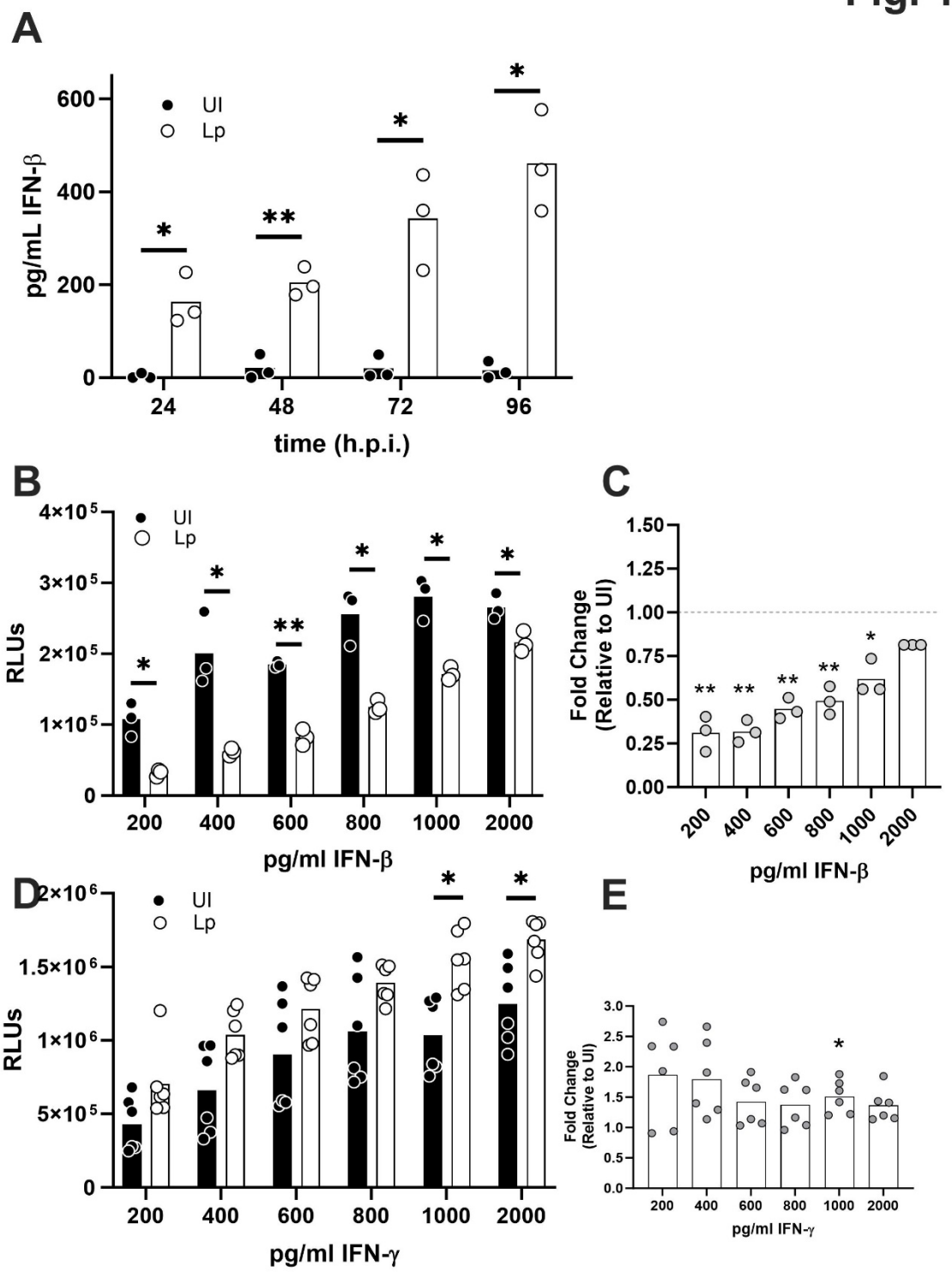
A
UI
Lp
pg/mL IFN-β
600
400
200
0
24
48
72
96
time (h.p.i.)
B
UI
Lp
RLUs
4×10⁵
3×10⁵
2×10⁵
1×10⁵
0
200
400
600
800
1000
2000
pg/ml IFN-β
C
Fold Change
(Relative to UI)
1.50
1.25
1.00
0.75
0.50
0.25
0.00
200
400
600
800
1000
2000
pg/ml IFN-β
D
UI
Lp
RLUs
2×10⁶
1.5×10⁶
1×10⁶
5×10⁵
0
200
400
600
800
1000
2000
pg/ml IFN-γ
E
Fold Change
(Relative to UI)
3.0
2.5
2.0
1.5
1.0
0.5
0.0
200
400
600
800
1000
2000
pg/ml IFN-γ

479 **Figure 1: *Legionella pneumophila* inhibits type I but not type II IFN signaling.** (A) RAW-
480 Lucia ISG-KO-IRF3 cells were infected with *L. pneumophila* (Lp) at an MOI of 0.05, and the
481 amount of secreted IFN-β was detected by ELISA. (B) Infected (Lp) (MOI of 10) and uninfected
482 (UI) cells were challenged with increasing concentrations of IFN-β, and the IFN-β/γ-signaling
483 reporter gene expression was measured after 20 hours post-infection (h.p.i.) by detection of
484 secreted luciferase into the supernatant and values are plotted as relative light units (RLU). (C)
485 The data in B was expressed as the fold change of Lp-infected, IFN-β-treated cells compared to
486 uninfected, IFN-β-treated cells. (D) Infected (MOI of 10) and uninfected cells were challenged
487 with increasing concentrations of IFN-γ, and the IFN-β/γ-signaling reporter gene expression was
488 measured after 20 h.p.i. as for B. (E) The data in D was expressed as the fold change of Lp-
489 infected, IFN- γ-treated cells compared to uninfected, IFN- γ-treated cells. Individual points are
490 from independent experiments and indicate the averages of three technical replicates. Statistical
491 analyses were done using multiple unpaired *t*-tests with Welch correction for each time point (A)
492 or each dose concentration of IFN-β or IFN-γ (B, D). The fold change is relative to the uninfected
493 cells for the same IFN-β or IFN-γ treatment concentration. Statistical analyses were done using
494 multiple unpaired *t*-tests with Welch correction, and each fold change was compared to the fold
495 change of the uninfected cells for each treatment dose of IFN-β or IFN-γ (C, E). Significance is
496 indicated as follows: *$p \leq 0.05$ and **$p \leq 0.01$.
497

Fig. 2

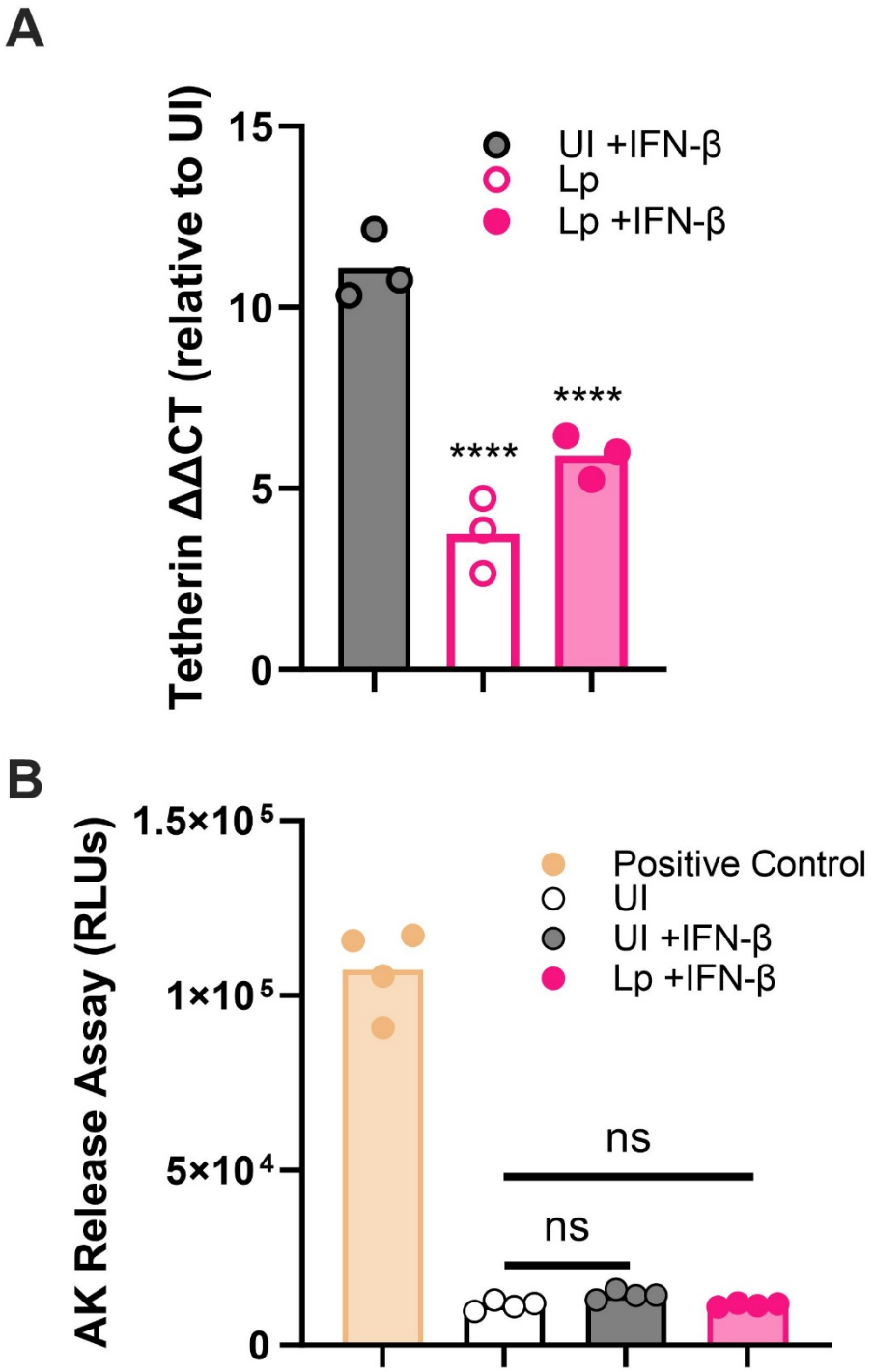
A
Tetherin ΔΔCT (relative to UI)
15
10
5
0
UI +IFN-β
Lp
Lp +IFN-β
****
****
B
AK Release Assay (RLUs)
1.5×10⁵
1×10⁵
5×10⁴
0
Positive Control
UI
UI +IFN-β
Lp +IFN-β
ns
ns

498

499 **Figure 2: *L. pneumophila* (Lp) infection decreases transcriptional response to IFN-β-**
500 **treatment without affecting cell death.** (A) Tetherin mRNA expression of RAW-Lucia ISG-KO-
501 IRF3 cells was quantified via qRT-PCR in *L. pneumophila* (Lp)-infected/untreated cells, Lp-
502 infected/IFN-β-treated cells and uninfected (UI)/IFN-β-treated cells at 4 hours post infection
503 (h.p.i.) and expressed as fold change compared to uninfected, untreated cells. The cells were
504 infected with Lp at an MOI of 10. (B) RAW-Lucia ISG-KO-IRF3 cell death was measured by an
505 adenylate kinase release assay in cells infected or not with *L. pneumophila* at an MOI of 10 after
506 20 h.p.i. and expressed as relative light units (RLU). The positive control is cells lysed with a
507 detergent. For A and B, individual points are the averages of three technical repeats and
508 obtained from independent experiments. An asterisk indicates multiple unpaired *t*-tests with
509 Welch correction relative to the untreated cells. Significance is indicated as follows: ****$p \leq$
510 0.0001.
511
512

Fig. 3

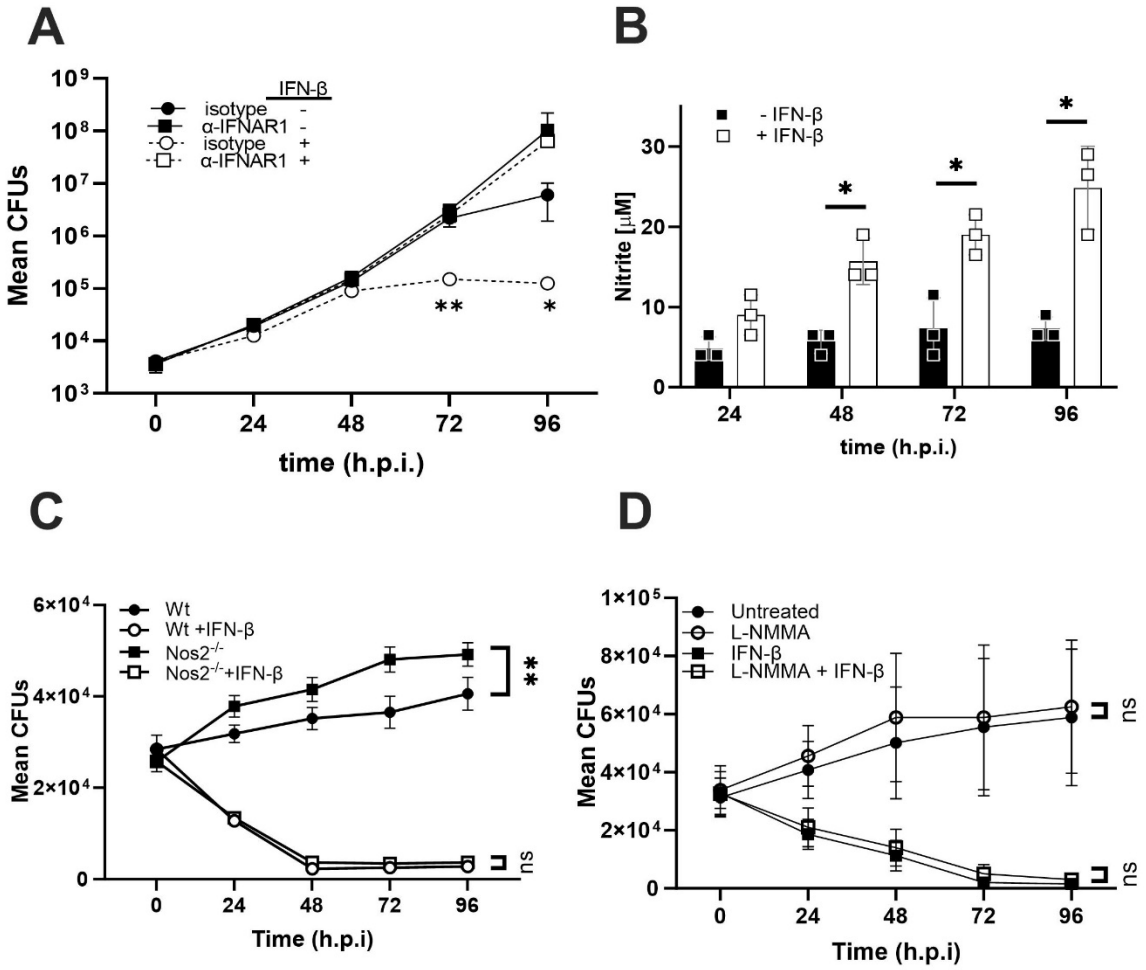
A
IFN-β
isotype -
α-IFNAR1 -
isotype +
α-IFNAR1 +
Mean CFUs
time (h.p.i.)
B
- IFN-β
+ IFN-β
Nitrite [μM]
time (h.p.i.)
C
Wt
Wt +IFN-β
Nos2-/-
Nos2-/-+IFN-β
Mean CFUs
Time (h.p.i)
ns
D
Untreated
L-NMMA
IFN-β
L-NMMA + IFN-β
Mean CFUs
Time (h.p.i)
ns

513

514

515 **Figure 3: IFN-β-treatment increases cell-intrinsic resistance to *L. pneumophila***
516 **independent of NO production.** (A) Bone marrow-derived macrophages (BMDMs) from *Ifnb*$^{-/-}$
517 mice were infected with *L. pneumophila* (Lp) at an MOI of 1 and treated with 1000 pg/ml IFN-
518 β throughout the infection. The number of colony-forming units (CFUs) was counted at the
519 indicated time points. The data are the mean ± standard deviation of six replicates obtained
520 from two independent infections. Asterisks indicate multiple unpaired *t*-tests with Welch
521 correction relative to the untreated cells. (B) RAW-ISG-KO-IRF3 cells were infected with Lp at
522 an MOI of 10. The amount of produced nitrite was measured using a Griess assay and shown
523 as the averages of three technical replicate from three independent experiments. (C) BMDMs
524 from *Nos2*$^{-/-}$ mice were infected with Lp at an MOI of 1 and treated with 1000 pg/ml IFN-
525 β throughout the infection. The number of CFUs was counted at the indicated time points. The
526 points are the mean ± standard deviation of three independent experiments. Asterisks indicate
527 multiple unpaired *t*-tests with Welch correction relative to the untreated cells. (D) Wildtype
528 BMDM cells were infected with Lp at MOI of 1 and treated with 1000 pg/ml IFN-β and solvent
529 control (DMSO) or L-NMMA (12 μM). The mean ± standard deviation of three independent
530 experiments are shown. Asterisks indicate a multiple unpaired *t*-test with Welch correction
531 comparing DMSO ± IFN-β or L-NMMA ± IFN-β. Significance is indicated as follows: *$p \leq 0.05$
532 and **$p \leq 0.01$.
533

Fig. 4

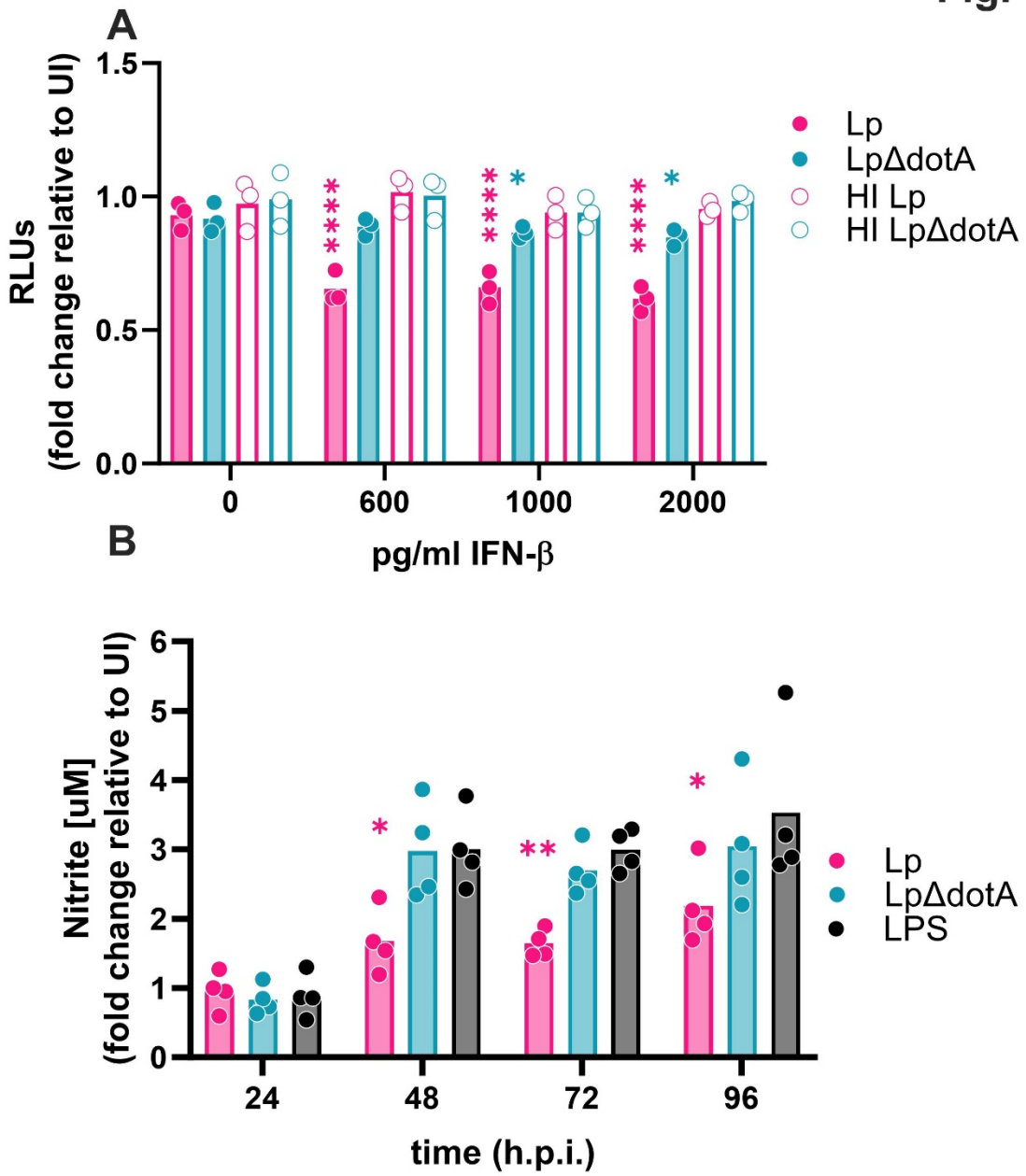
A
RLUs
(fold change relative to UI)
1.5
1.0
0.5
0.0
0
600
1000
2000
pg/ml IFN-β
Lp
LpΔdotA
HI Lp
HI LpΔdotA
B
Nitrite [uM]
(fold change relative to UI)
6
5
4
3
2
1
0
24
48
72
96
time (h.p.i.)
Lp
LpΔdotA
LPS

534

535

536 **Figure 4: The inhibition of IFN-β signaling by *L. pneumophila* is dependent on its type IV**
537 **secretion system.** (A) RAW-ISG-KO-IRF3 cells were infected with wild-type *L. pneumophila*
538 (Lp), the Lp *dotA* deficient mutant (Lp∆*dotA*), the heat-inactivated wild-type Lp (HI Lp), or the
539 heat-inactivated *dotA* deficient mutant (HI Lp∆*dotA*) at an MOI of 10. All experimental groups
540 were treated with the indicated amounts of IFN-β. The y-axis shows the fold change in IFN-β
541 reporter gene expression compared to the uninfected/untreated experimental group after 20
542 h.p.i.. Data points are from independent experiments and represent the averages of three
543 technical replicates. (B) RAW-ISG-KO-IRF3 cells were infected with wild-type Lp or the Lp *dotA*
544 deficient mutant (Lp∆*dotA*) at an MOI of 10 or left uninfected but treated with LPS (100 ng/ml).
545 All cells were treated with 1000 pg/ml IFN-β. The production of NO was measured via the
546 Griess assay at the indicated times, and the data points from independent experiments and the
547 averages of three technical replicates. The data is expressed as fold change compared to
548 uninfected/treated cells. A two-way ANOVA with Geisser-Greenhouse correction and Tukey's
549 multiple comparisons test was performed on all data. Significance is indicated as follows: *$p \leq$
550 0.05, **$p \leq 0.01$, and ****$p \leq 0.0001$.
551
552

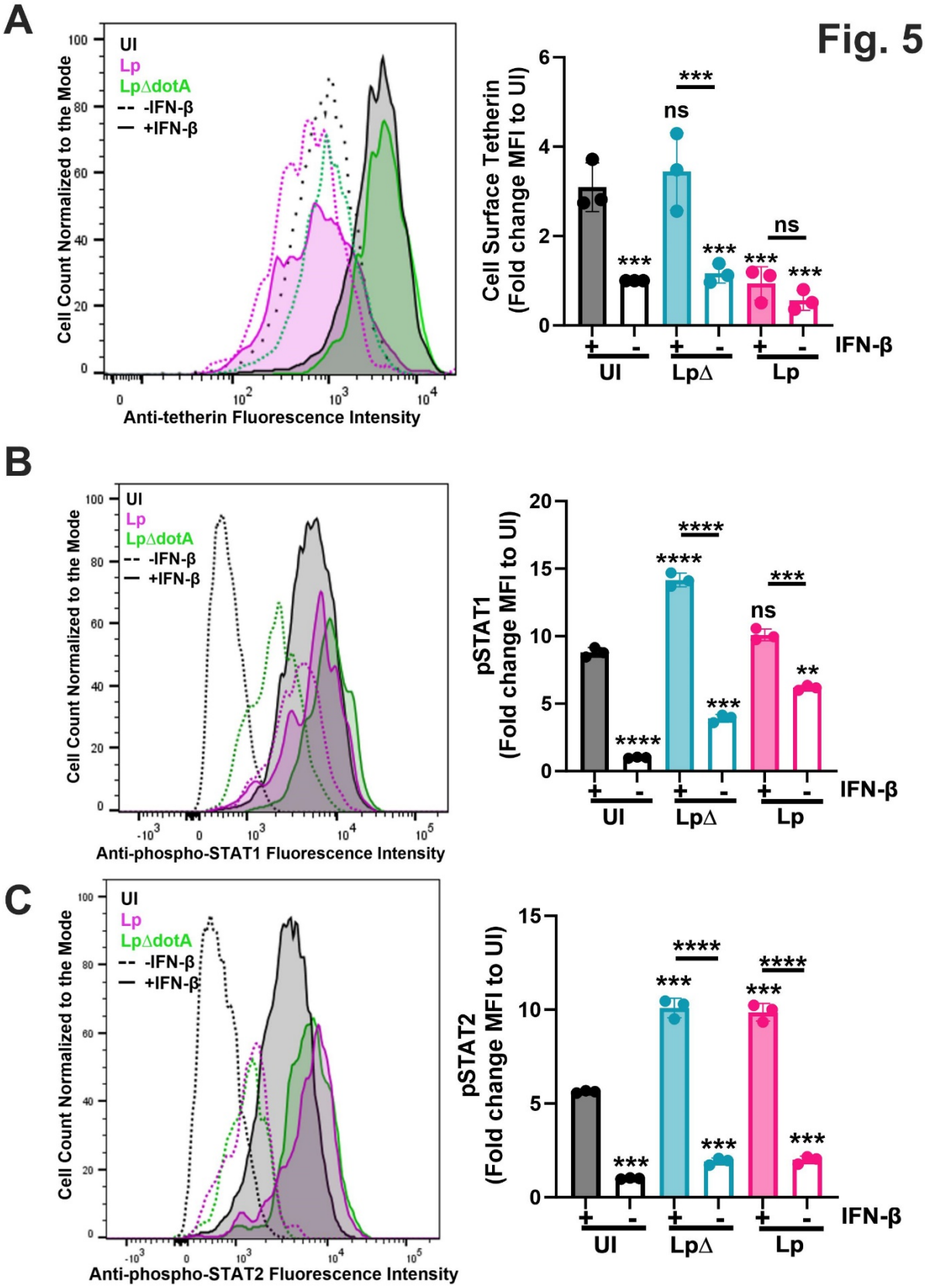
Fig. 5
A
UI
Lp
LpΔdotA
-- -IFN-β
— +IFN-β
Cell Count Normalized to the Mode
Anti-tetherin Fluorescence Intensity
Cell Surface Tetherin
(Fold change MFI to UI)
ns
***
IFN-β
UI
LpΔ
Lp
B
Anti-phospho-STAT1 Fluorescence Intensity
pSTAT1
(Fold change MFI to UI)
****
**
C
Anti-phospho-STAT2 Fluorescence Intensity
pSTAT2
(Fold change MFI to UI)

553

554 **Figure 5: *L. pneumophila* inhibits cell surface expression of tetherin but does not affect**
555 **the phosphorylation of STAT1 and STAT2.** THP-1 cells were infected with GFP-expressing
556 wild-type *L. pneumophila* (Lp) and *dotA* deficient mutant (LpΔ) at an MOI of 10 and treated or
557 not with 10 ng/ml IFN-β. (A) The flow cytometry analysis performed on the GFP+/infected cells
558 using a fluorescent antibody targeting the cell surface ISG protein tetherin at 20 h.p.i.. (B) The
559 flow cytometry analysis performed on the GFP+/infected cells at an MOI of 10 using a
560 fluorescent antibody targeting phosphorylated STAT1 30 minutes post infection. (C) The flow
561 cytometry analysis performed on the GFP+/infected cells at an MOI of 10 using a fluorescent
562 antibody targeting phosphorylated STAT2 30 minutes post infection. The histograms are from
563 one experiment representative of three independent experiments. The bar graphs show the
564 mean fluorescent intensity (MFI) fold changes compared with the uninfected untreated cells for
565 each flow cytometry analysis. Individual points represent independent experiments. An asterisk
566 indicates multiple unpaired *t*-tests with Welch correction relative to the uninfected IFN-β treated
567 cells. Significance is indicated as follows: $^{**}p \leq 0.01$, $^{***}p \leq 0.001$, and $^{****}p \leq 0.0001$.
568
569

Sup Fig. 1

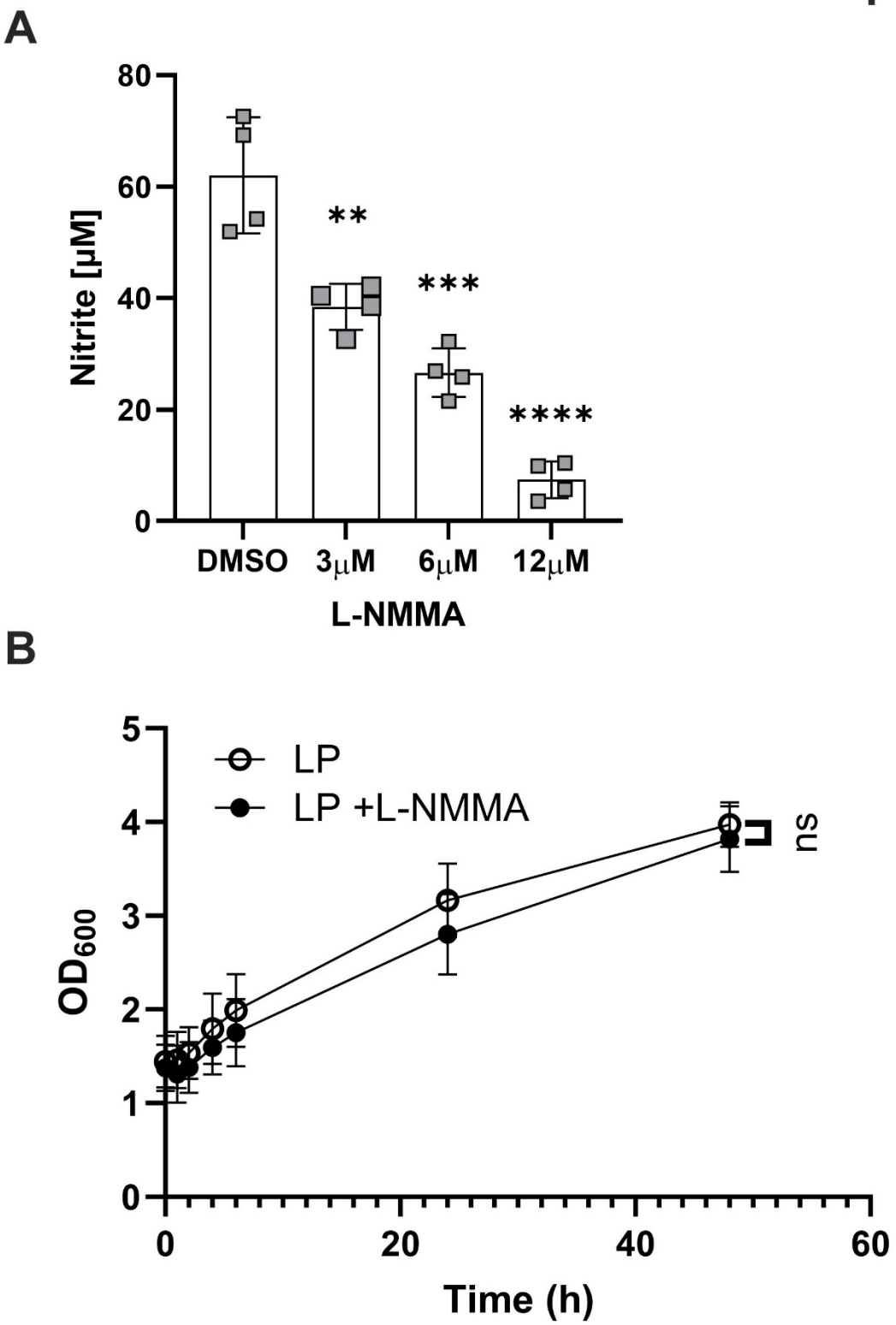
A
80
60
40
20
0
Nitrite [μM]
**
***
****
DMSO
3μM
6μM
12μM
L-NMMA
B
5
4
3
2
1
0
OD600
LP
LP +L-NMMA
ns
0
20
40
60
Time (h)

570

571 **Supplementary Figure 1: Effects of L-NMMA on nitrite production and *L. pneumophila***
572 **growth.** (A) The dose-response analysis of the iNOS2 inhibitor L-NMMA on RAW-ISG-KO-IRF3
573 cells treated with 1000 pg/ml of IFN-β 20 hours after dosing. The data points are from four
574 independent experiments. The statistical analysis was done using a repeat-measure (RM) one-
575 way ANOVA. (B) The growth curve of wild-type *L. pneumophila* (Lp) measured by OD_{600} in the
576 presence or absence of 12 μM L-NMMA. Points are the averages mean ± standard deviation of
577 three independent experiments. The statistical analysis was done by a multiple unpaired *t*-test
578 with Welch correction comparing the two groups at the time points indicated. Significance is
579 indicated as follows: $^{**}p \leq 0.01$, $^{***}p \leq 0.001$, and $^{****}p \leq 0.0001$.
580
581

Sup Fig. 2

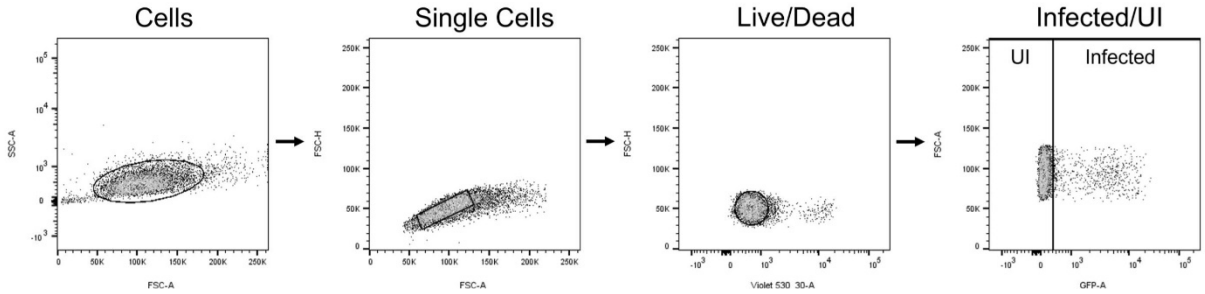
Cells
Single Cells
Live/Dead
Infected/UI
UI
Infected
SSC-A
FSC-A
FSC-H
Violet 530 30-A
GFP-A

582

583 **Supplementary Figure 2: Flow Cytometry Gating Strategy.** THP-1 cells were first gated to
584 isolate cells from debris (SSC/FSC). Next single cells were selected (FSC-H/FSC-A) and using
585 LIVE/DEAD Fixable Dye the live cells were selected. Lastly, infected cells were selected by
586 measuring the GFP fluorescence intensity.
587

Sup Fig. 3

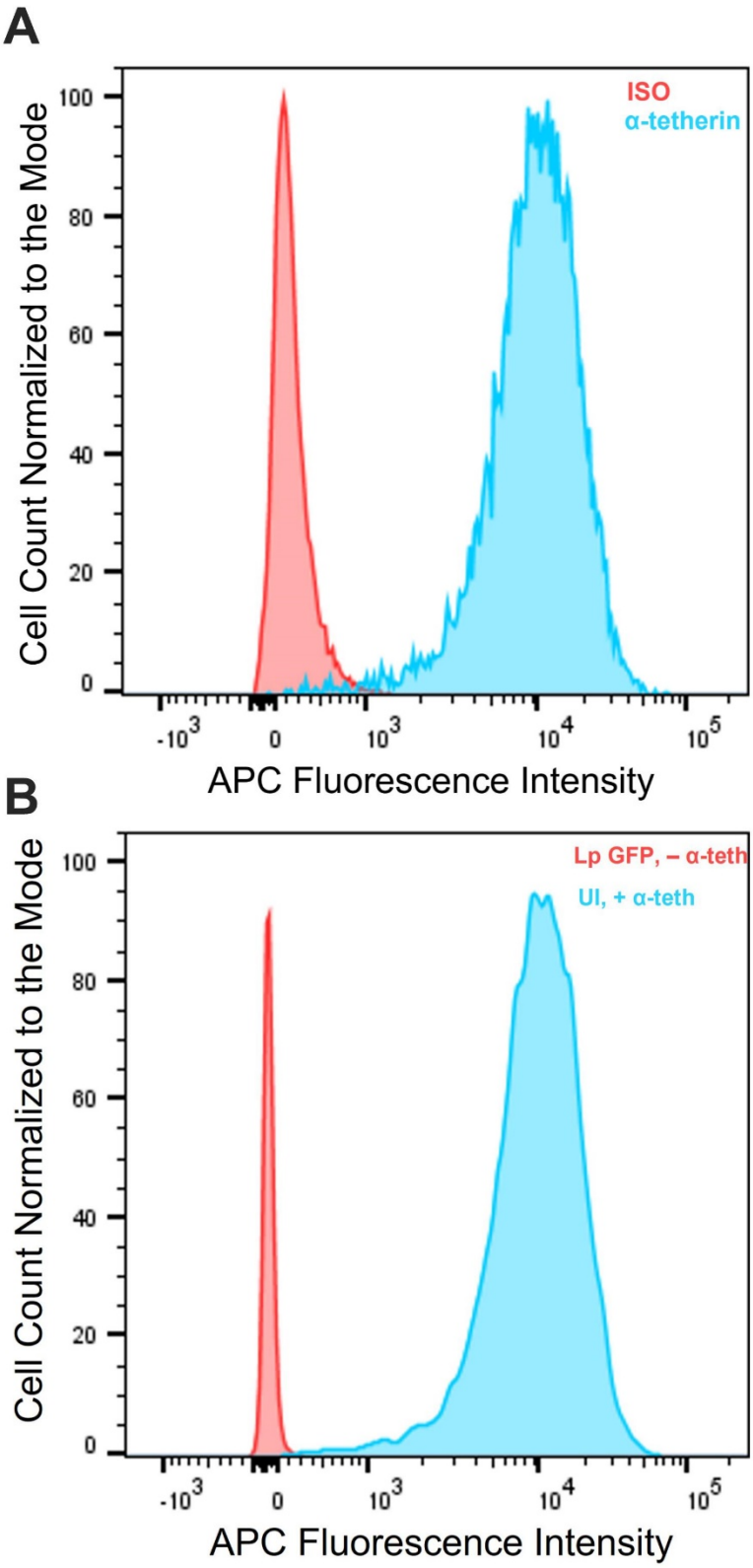
A
ISO
α-tetherin
Cell Count Normalized to the Mode
100
80
60
40
20
0
-10^3
0
10^3
10^4
10^5
APC Fluorescence Intensity
B
Lp GFP, – α-teth
UI, + α-teth
Cell Count Normalized to the Mode
100
80
60
40
20
0
-10^3
0
10^3
10^4
10^5
APC Fluorescence Intensity

588

589 **Supplementary Figure 3: Tetherin antibody testing and GFP Flow Cytometry.** (A) MFI
590 peaks of uninfected IFN-β (10 ng/ml) treated THP-1 cells stained with the tetherin (α-tetherin) or
591 Isotype control antibodies (ISO). (B) Histograms of uninfected THP-1 cells stained with the APC
592 conjugated tetherin antibody (UI+IFN-β) and *L. pneumophila* GFP infected (GFP) (MOI of 10)
593 unstained cells measuring the APC intensity.
594
595

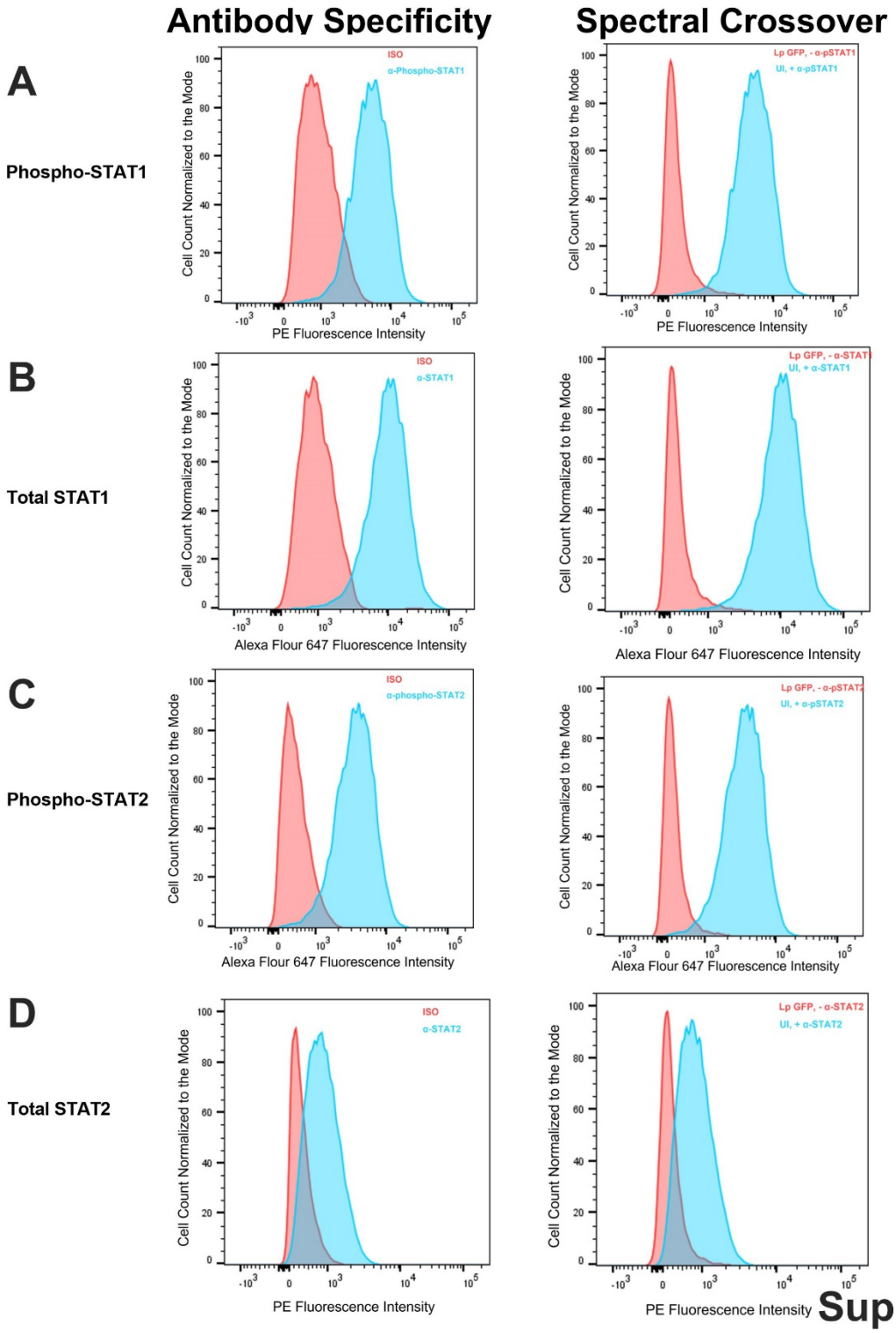
Antibody Specificity
Spectral Crossover
A
Phospho-STAT1
B
Total STAT1
C
Phospho-STAT2
D
Total STAT2
ISO
α-Phospho-STAT1
α-STAT1
α-phospho-STAT2
α-STAT2
Lp GFP, - α-pSTAT1
UI, + α-pSTAT1
Lp GFP, - α-STAT1
UI, + α-STAT1
Lp GFP, - α-pSTAT2
UI, + α-pSTAT2
Lp GFP, - α-STAT2
UI, + α-STAT2
Cell Count Normalized to the Mode
PE Fluorescence Intensity
Alexa Flour 647 Fluorescence Intensity

Sup Fig. 4

596

597 **Supplementary Figure 4: Isotype antibodies and GFP Flow Cytometry control**
598 **experiments.** The left column indicates the tests of the specific antibody stainings compared to
599 isotype controls as indicated and uninfected/IFN-β-treated (10 ng/ml) THP1 cells. The right
600 column analyses the potential spectral crossover of the GFP-signal into any of the other
601 channels used for the specific antibody stainings by infecting cells with Lp-GFP (MOI of 10) and
602 no specific antibody or having uninfected/IFN-β-treated cells stained with specific antibody. (A)
603 phospho-STAT1 antibody (B) total STAT1 antibody, (C) phospho-STAT2 antibody and (D) total
604 STAT2 antibody.
605

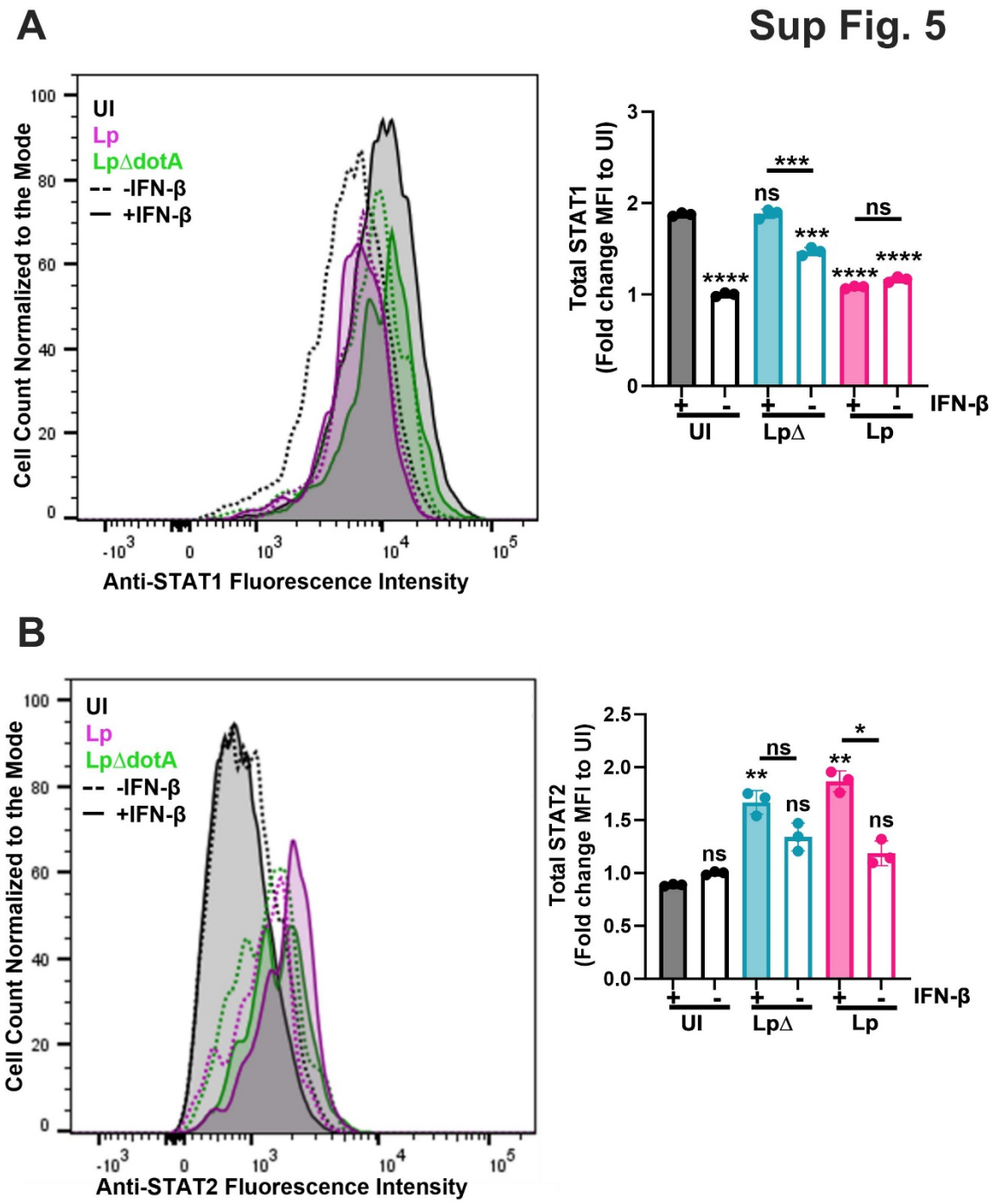
A
Sup Fig. 5
UI
Lp
LpΔdotA
-- -IFN-β
— +IFN-β
Cell Count Normalized to the Mode
Anti-STAT1 Fluorescence Intensity
Total STAT1
(Fold change MFI to UI)
IFN-β
UI
LpΔ
Lp
B
Anti-STAT2 Fluorescence Intensity
Total STAT2
(Fold change MFI to UI)

606

607 **Supplementary Figure 5: The effects of *L. pneumophila* infection on the total STAT1 and**
608 **STAT2 levels.** THP-1 cells were infected with GFP-expressing wild-type *L. pneumophila* (Lp)
609 and *dotA* deficient mutant (LpΔ) at an MOI of 10. The treated groups were treated with 10 ng/ml
610 IFN-β. (A) The flow cytometry analysis performed on the GFP+ infected cells using a fluorescent
611 antibody targeting total STAT1 30 minutes post infection. (B) The flow cytometry analysis
612 performed on the GFP+ infected cells using a fluorescent antibody targeting total STAT2 30
613 minutes post infection. The histograms are representative of three independent experiments
614 and illustrate the mean fluorescent intensity (MFI) of each group. The bar graphs show the MFI
615 fold changes compared with the uninfected/ untreated cells for each flow cytometry analysis.
616 Individual points indicate independent experiments. An asterisk indicates multiple unpaired *t*-
617 tests with Welch correction relative to the uninfected IFN-β treated cells. Significance is
618 indicated as follows: *$p \leq 0.05$, **$p \leq 0.01$, ***$p \leq 0.001$, and ****$p \leq 0.0001$.
619
620

621 **References**

622
623

624 Abdul-Sater, A. A., Majoros, A., Plumlee, C. R., Perry, S., Gu, A.-D., Lee, C., et al. (2015). Different
625 STAT Transcription Complexes Drive Early and Delayed Responses to Type I IFNs. *J Immunol* 195,
626 210--216. doi: 10.4049/jimmunol.1401139.

627 Akamine, M., Higa, F., Haranaga, S., Tateyama, M., Mori, N., Heuner, K., et al. (2007). Interferon-
628 Gamma Reverses the Evasion of Birc1e/Naip5 Gene Mediated Murine Macrophage Immunity by
629 Legionella pneumophila Mutant Lacking Flagellin. *Microbiol. Immunol.* 51, 279–287. doi:
630 10.1111/j.1348-0421.2007.tb03909.x.

631 Allegra, S., Grattard, F., Girardot, F., Riffard, S., Pozzetto, B., and Berthelot, P. (2011). Longitudinal
632 Evaluation of the Efficacy of Heat Treatment Procedures against Legionella spp. in Hospital Water
633 Systems by Using a Flow Cytometric Assay. *Appl. Environ. Microbiol.* 77, 1268–1275. doi:
634 10.1128/aem.02225-10.

635 Alphonse, N., Wanford, J. J., Voak, A. A., Gay, J., Venkhaya, S., Burroughs, O., et al. (2022). A family
636 of conserved bacterial virulence factors dampens interferon responses by blocking calcium signaling.
637 *Cell* 185, 2354-2369.e17. doi: 10.1016/j.cell.2022.04.028.

638 Banks, D. A., Ahlbrand, S. E., Hughitt, V. K., Shah, S., Mayer-Barber, K. D., Vogel, S. N., et al. (2019a).
639 Mycobacterium tuberculosis Inhibits Autocrine Type I IFN Signaling to Increase Intracellular
640 Survival. *Journal of immunology (Baltimore, Md. : 1950)*, ji1801303. doi:
641 10.4049/jimmunol.1801303.

642 Banks, D. A., Ahlbrand, S. E., Hughitt, V. K., Shah, S., Mayer-Barber, K. D., Vogel, S. N., et al. (2019b).
643 Mycobacterium tuberculosis Inhibits Autocrine Type I IFN Signaling to Increase Intracellular
644 Survival. *Journal of immunology (Baltimore, Md. : 1950)*, ji1801303. doi:
645 10.4049/jimmunol.1801303.

646 Belyi, Y., Niggeweg, R., Opitz, B., Vogelsgesang, M., Hippenstiel, S., Wilm, M., et al. (2006). Legionella
647 pneumophila glucosyltransferase inhibits host elongation factor 1A. *Proc. Natl. Acad. Sci.* 103,
648 16953–16958. doi: 10.1073/pnas.0601562103.

649 Berger, K. H., and Isberg, R. R. (1993). Two distinct defects in intracellular growth complemented by a
650 single genetic locus in Legionella pneumophila. *Mol Microbiol* 7, 7–19. doi: 10.1111/j.1365-
651 2958.1993.tb01092.x.

652 Boamah, D. K., Zhou, G., Ensminger, A. W., and O'Connor, T. J. (2017). From Many Hosts, One
653 Accidental Pathogen: The Diverse Protozoan Hosts of Legionella. *Front Cell Infect Mi* 7, 477. doi:
654 10.3389/fcimb.2017.00477.

655 Boxx, G. M., and Cheng, G. (2016). The Roles of Type I Interferon in Bacterial Infection. *Cell Host and*
656 *Microbe* 19, 760–769. doi: 10.1016/j.chom.2016.05.016.

657 Brand, B. C., Sadosky, A. B., and Shuman, H. A. (1994). The Legionella pneumophila icm locus: a set of
658 genes required for intracellular multiplication in human macrophages. *Mol Microbiol* 14, 797–808.
659 doi: 10.1111/j.1365-2958.1994.tb01316.x.

660 Deonarain, R., Alcami, A., Alexiou, M., Dallman, M. J., Gewert, D. R., and Porter, A. C. G. (2000).
661 Impaired Antiviral Response and Alpha/Beta Interferon Induction in Mice Lacking Beta Interferon.
662 *Journal of Virology* 74, 3404–3409. doi: 10.1128/jvi.74.7.3404-3409.2000.

663 Fontana, M. F., Banga, S., Barry, K. C., Shen, X., Tan, Y., Luo, Z.-Q., et al. (2011). Secreted Bacterial
664 Effectors That Inhibit Host Protein Synthesis Are Critical for Induction of the Innate Immune
665 Response to Virulent Legionella pneumophila. *Plos Pathog* 7, e1001289. doi:
666 10.1371/journal.ppat.1001289.

667 Gebran, S. J., Yamamoto, Y., Newton, C., Klein, T. W., and Friedman, H. (1994). Inhibition of
668 Legionella pneumophila growth by gamma interferon in permissive A/J mouse macrophages: role of
669 reactive oxygen species, nitric oxide, tryptophan, and iron(III). *Infect. Immun.* 62, 3197–3205. doi:
670 10.1128/iai.62.8.3197-3205.1994.

671 Gilchrist, A. K., Smolensky, D., Ngwaga, T., Chauhan, D., Cox, S., Perumal, R., et al. (2020). High-
672 polyphenol extracts from Sorghum bicolor attenuate replication of Legionella pneumophila within
673 RAW 264.7 macrophages. *Fems Microbiol Lett* 367, fnaa053. doi: 10.1093/femsle/fnaa053.

674 Goldberg, J. M., Manning, G., Liu, A., Fey, P., Pilcher, K. E., Xu, Y., et al. (2006). The Dictyostelium
675 Kinome—Analysis of the Protein Kinases from a Simple Model Organism. *Plos Genet* 2, e38. doi:
676 10.1371/journal.pgen.0020038.

677 Jacobs, A. T., and Ignarro, L. J. (2001). Lipopolysaccharide-induced Expression of Interferon-β Mediates
678 the Timing of Inducible Nitric-oxide Synthase Induction in RAW 264.7 Macrophages*. *J Biol Chem*
679 276, 47950–47957. doi: 10.1074/jbc.m106639200.

680 Kaneko, T., Stogios, P. J., Ruan, X., Voss, C., Evdokimova, E., Skarina, T., et al. (2018). Identification
681 and characterization of a large family of superbinding bacterial SH2 domains. *Nat. Commun.* 9, 4549.
682 doi: 10.1038/s41467-018-06943-2.

683 Kawata, T., Shevchenko, A., Fukuzawa, M., Jermyn, K. A., Totty, N. F., Zhukovskaya, N. V., et al.
684 (1997). SH2 Signaling in a Lower Eukaryote: A STAT Protein That Regulates Stalk Cell
685 Differentiation in Dictyostelium. *Cell* 89, 909–916. doi: 10.1016/s0092-8674(00)80276-7.

686 Kicinska, A., Leluk, J., and Jarmuszkiewicz, W. (2014). Acanthamoeba castellanii STAT Protein. *Plos*
687 *One* 9, e111345. doi: 10.1371/journal.pone.0111345.

688 Lazear, H. M., Schoggins, J. W., and Diamond, M. S. (2019). Shared and Distinct Functions of Type I
689 and Type III Interferons. *Immunity* 50, 907–923. doi: 10.1016/j.immuni.2019.03.025.

690 Lippmann, J., Müller, H. C., Naujoks, J., Tabeling, C., Shin, S., Witzenrath, M., et al. (2011). Dissection
691 of a type I interferon pathway in controlling bacterial intracellular infection in mice. *Cell Microbiol*
692 13, 1668–1682. doi: 10.1111/j.1462-5822.2011.01646.x.

693 Liu, M., Conover, G. M., and Isberg, R. R. (2008). Legionella pneumophila EnhC is required for efficient
694 replication in tumour necrosis factor α-stimulated macrophages. *Cell Microbiol* 10, 1906–1923. doi:
695 10.1111/j.1462-5822.2008.01180.x.

696 Liu, X., and Shin, S. (2019). Viewing Legionella pneumophila pathogenesis through an immunological
697 lens. *J Mol Biol* 431, 4321–4344. doi: 10.1016/j.jmb.2019.07.028.

698 Majoros, A., Platanitis, E., Szappanos, D., Cheon, H., Vogl, C., Shukla, P., et al. (2016). Response to
699 interferons and antibacterial innate immunity in the absence of tyrosine-phosphorylated STAT1. *Embo*
700 *Rep* 17, 367–382. doi: 10.15252/embr.201540726.

701 McDade, J. E., Shepard, C. C., Fraser, D. W., Tsai, T. R., Redus, M. A., and Dowdle, W. R. (1977).
702 Legionnaires' Disease — Isolation of a Bacterium and Demonstration of Its Role in Other Respiratory
703 Disease. *New Engl J Medicine* 297, 1197–1203. doi: 10.1056/nejm197712012972202.

704 Monroe, K. M., McWhirter, S. M., and Vance, R. E. (2009). Identification of Host Cytosolic Sensors and
705 Bacterial Factors Regulating the Type I Interferon Response to Legionella pneumophila. *Plos Pathog*
706 5, e1000665. doi: 10.1371/journal.ppat.1000665.

707 Moss, S. M., Taylor, I. R., Ruggero, D., Gestwicki, J. E., Shokat, K. M., and Mukherjee, S. (2019). A
708 Legionella pneumophila Kinase Phosphorylates the Hsp70 Chaperone Family to Inhibit Eukaryotic
709 Protein Synthesis. *Cell Host Microbe* 25, 454-462.e6. doi: 10.1016/j.chom.2019.01.006.

710 Naujoks, J., Tabeling, C., Dill, B. D., Hoffmann, C., Brown, A. S., Kunze, M., et al. (2016). IFNs Modify
711 the Proteome of Legionella-Containing Vacuoles and Restrict Infection Via IRG1-Derived Itaconic
712 Acid. *PLoS Pathog.* 12, e1005408. doi: 10.1371/journal.ppat.1005408.

713 Opitz, B., Vinzing, M., Laak, V. van, Schmeck, B., Heine, G., Günther, S., et al. (2006). Legionella
714 pneumophila Induces IFNβ in Lung Epithelial Cells via IPS-1 and IRF3, Which Also Control
715 Bacterial Replication. *J Biol Chem* 281, 36173–36179. doi: 10.1074/jbc.m604638200.

716 Park, J. M., Ghosh, S., and O'Connor, T. J. (2020). Combinatorial selection in amoebal hosts drives the
717 evolution of the human pathogen Legionella pneumophila. *Nat Microbiol* 5, 599–609. doi:
718 10.1038/s41564-019-0663-7.

719 Peignier, A., and Parker, D. (2021). Impact of Type I Interferons on Susceptibility to Bacterial Pathogens.
720 *Trends in microbiology*, 1–13. doi: 10.1016/j.tim.2021.01.007.

721 Plumlee, C. R., Lee, C., Beg, A. A., Decker, T., Shuman, H. A., and Schindler, C. (2009). Interferons
722 Direct an Effective Innate Response to Legionella pneumophila Infection*. *J Biol Chem* 284, 30058–
723 30066. doi: 10.1074/jbc.m109.018283.

724 Price, J. V., Russo, D., Ji, D. X., Chavez, R. A., DiPeso, L., Lee, A. Y.-F., et al. (2019). IRG1 and
725 Inducible Nitric Oxide Synthase Act Redundantly with Other Interferon-Gamma-Induced Factors To
726 Restrict Intracellular Replication of Legionella pneumophila. *Mbio* 10, e02629-19. doi:
727 10.1128/mbio.02629-19.

728 Rowbotham, T. J. (1980). Preliminary report on the pathogenicity of Legionella pneumophila for
729 freshwater and soil amoebae. *J Clin Pathol* 33, 1179. doi: 10.1136/jcp.33.12.1179.

730 Schiavoni, G., Mauri, C., Carlei, D., Belardelli, F., Pastoris, M. C., and Proietti, E. (2004). Type I IFN
731 Protects Permissive Macrophages from Legionella pneumophila Infection through an IFN-γ-
732 Independent Pathway. *J Immunol* 173, 1266–1275. doi: 10.4049/jimmunol.173.2.1266.

733 Schlessinger, J., and Lemmon, M. A. (2003). SH2 and PTB Domains in Tyrosine Kinase Signaling. *Sci.'s*
734 *STKE* 2003, RE12. doi: 10.1126/stke.2003.191.re12.

735 Segal, G., and Shuman, H. A. (1998). Intracellular multiplication and human macrophage killing by
736 Legionella pneumophila are inhibited by conjugal components of IncQ plasmid RSF1010. *Mol*
737 *Microbiol* 30, 197–208. doi: 10.1046/j.1365-2958.1998.01054.x.

738 Shen, X., Banga, S., Liu, Y., Xu, L., Gao, P., Shamovsky, I., et al. (2009). Targeting eEF1A by a
739 Legionella pneumophila effector leads to inhibition of protein synthesis and induction of host stress
740 response. *Cell. Microbiol.* 11, 911–926. doi: 10.1111/j.1462-5822.2009.01301.x.

741 Stetson, D. B., and Medzhitov, R. (2006). Type I interferons in host defense. *Immunity* 25, 373–381. doi:
742 10.1016/j.immuni.2006.08.007.

743 Villarino, A. V., Gadina, M., O'Shea, J. J., and Kanno, Y. (2020). SnapShot: Jak-STAT Signaling II. *Cell*
744 181, 1696-1696.e1. doi: 10.1016/j.cell.2020.04.052.

745 Vogel, Joseph. P., Andrews, H. L., Wong, S. K., and Isberg, R. R. (1998). Conjugative Transfer by the
746 Virulence System of Legionella pneumophila. *Science* 279, 873–876. doi:
747 10.1126/science.279.5352.873.

748